Journal of Non-Newtonian Fluid Mechanics 234 (2016) 69–81

Contents lists available at ScienceDirect

Journal of Non-Newtonian Fluid Mechanics

journal homepage: www.elsevier.com/locate/jnnfm

Viscoplastic flow development in tubes and channels with wall slip

Maria Philippou, Zacharias Kountouriotis, Georgios C. Georgiou*

Department of Mathematics and Statistics, University of Cyprus, P.O. Box 20537, 1678 Nicosia, Cyprus

ARTICLE INFO

Article history:
Received 15 February 2016
Revised 15 April 2016
Accepted 20 April 2016
Available online 22 April 2016

Keywords:
Bingham plastic
Papanastasiou regularization
Wall slip
Poiseuille flow
Development length

ABSTRACT

The development of Bingham plastic flow in tubes and channels is investigated numerically using the Papanastasiou regularization and finite element simulations. It is assumed that slip occurs along the wall following Navier's law, according to which the slip velocity varies linearly with the wall shear stress. Alternative definitions of the development length are discussed and the combined effects of slip and yield stress at low and moderate Reynolds numbers are investigated. It is demonstrated that even for the Newtonian channel flow using the conventional centreline development length is not a good choice when slip is present. Similarly, the development length definition proposed by Ookawara et al. [J. Chem. Eng. Japan 33, 675-678 (2000)] for viscoplastic flows results in misleading conclusions regarding the effect of yield stress on flow development. To avoid such inconsistencies a global development length is employed. In general, the global development length is monotonically increasing with the Reynolds and Bingham numbers. As slip is increased, the latter length initially increases exhibiting a global maximum before vanishing rapidly slightly above the critical point corresponding to sliding flow.

1. Introduction

The Newtonian flow-development or entry-flow problem in tubes of various cross sections was studied systematically (experimentally and numerically) in the late 1960s and in the 1970s under the assumption that the fluid adheres to the wall [1-5]. However, the problem has been revisited by many investigators in the past few years due to its relevance in micro-/nano-fluidics and in biomechanics and the need to further investigate non-Newtonian, wall slip, and oscillatory flow effects [5–7]. Studies concerning the flow development of non-Newtonian flows have been reviewed by Tanner [8]. More recent studies include power–law fluids [6], Bingham plastic materials [9,10], Oldroyd-B and Phan-Thien-Tanner fluids [11], and Sisco fluids [12].

The development or entrance length, L^*, i.e. the length required for steady-state laminar pipe flow to fully develop from a uniform to the corresponding Poiseuille distribution, is the main parameter of interest. L^* is most commonly defined as the length required for the cross-sectional maximum velocity to attain 99% of its fully developed value [4]. This definition is obviously based on the assumption that the flow develops more slowly along the axis of symmetry than elsewhere. As discussed below, this is not always the case, especially in the presence of wall slip or with yield stress fluids. In general, the dimensionless development length is defined by $L \equiv L^*/L_s^*$, where L_s^* is a characteristic length, e.g. the diameter D^* for a pipe or the slit gap $2H^*$ for a channel. Note that throughout this paper dimensional quantities are denoted by starred symbols and thus symbols without stars correspond to dimensionless quantities and numbers.

As expected, the development length increases with inertia. In fact, the main concern in the Newtonian entry-flow literature was to obtain empirical correlations relating the development length to the Reynolds number, Re, with the emphasis given on moderate and high Reynolds numbers. As noted by Sinclair [5], the use of these correlations for low Reynolds numbers is questionable. It seems that the expressions proposed by Durst et al. [13], i.e.,

$$L = [(0.619)^{1.6} + (0.0567Re)^{1.6}]^{1/1.16} \quad \text{for pipe flow} \tag{1}$$

and

$$L = [(0.631)^{1.6} + (0.0442Re)^{1.6}]^{1/1.16} \quad \text{for channel flow} \tag{2}$$

are the most accurate. However, their predictions for zero Reynolds numbers are still only approximate. For example, their expression for a channel gives L=0.631 which disagrees with the extrapolated value of 0.6284 computed by Ferrás et al. [7] and the converged value of 0.6286 reported by Kountouriotis et al. [14].

Apart from inertia and geometry, other factors affecting the development length are wall slip and rheology. Wall slip can be important even in Newtonian entry flows in microfluidic and nanofluidic devices [15,16]. The effect of wall slip on the Newtonian flow development in a channel has been investigated numerically by

* Corresponding author. Tel.: +35722892612; fax: +35722895352.
E-mail address: georgios@ucy.ac.cy (G.C. Georgiou).

http://dx.doi.org/10.1016/j.jnnfm.2016.04.008
0377-0257/

Table 1
Characteristics of four uniform and four graded meshes with $L_{mesh} = 20$.

Mesh	Smallest element size	Number of elements	Number of nodes	Number of unknowns
M1	0.2	500	2211	5029
M2	0.1	2000	8421	19,054
M3	0.05	8000	32,841	74,104
M4	0.025	32,000	129,681	292,204
GM1	0.01	15,960	64,757	149,934
GM2	0.005	18,102	73,355	165,287
GM3	0.002	42,581	172,161	387,823
GM4	0.001	45,696	184,041	414,408

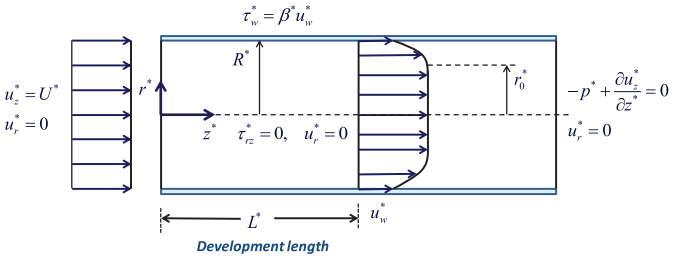

Fig. 1. Development of axisymmetric Poiseuille flow with wall slip: geometry and boundary conditions.

Ferrás et al. [7] by means of finite volume simulations. They employed the Navier-slip equation [17]:

$$\tau_w^* = \beta^* u_w^* \tag{3}$$

where τ_w^* is the wall shear stress, β^* is the slip coefficient, and u_w^* is the slip velocity. The latter is defined as the relative velocity of the fluid with respect to that of the wall. In general, the slip coefficient β^* incorporates the effects of temperature, normal stress and pressure, and the characteristics of the fluid/wall interface [18]. The no-slip boundary condition is recovered from Eq. (3) when $\beta^* \to \infty$. In the other extreme, i.e., when $\beta^* = 0$, the fluid slips perfectly.

Ferrás et al. [7] showed that the development length L initially increases and then decreases with wall slip (i.e. as β^* is reduced) exhibiting a maximum and that slip suppresses the velocity overshoots observed close to the wall near the entrance. They also extended the empirical expression of Durst et al. [13] for the development length in a channel including the slip parameter. Kountouriotis et al. [14] reproduced the results for the planar flow and solved the axisymmetric entry flow problem by means of finite elements. They also pointed out that, in addition to the classical centreline development length, a wall development length is also relevant in the presence of finite wall slip. They defined the wall development length, L_w, as the length required for the slip velocity to attain 101% of its fully developed value. In what follows, we will conveniently be using the symbol L_c for the classical development length. Kountouriotis et al. [14] showed that L_c is greater than L_w only in the axisymmetric flow. In the case of the channel flow, the wall development length is greater than the classical development length, which means that the flow development near the wall is slower. This effect becomes more pronounced at higher Reynolds numbers. Therefore, in the presence of wall slip, considering the classical definition of the development length is not always a safe criterion for assuring flow development across the pipe cross-section. As discussed below, this might also be the case if the fluid is not Newtonian.

In the present work, we are interested in viscoplastic materials, i.e. in materials with a yield-stress, which form a very large class including materials of industrial importance, such as suspensions,

Table 2
Various definitions of the development length in terms of the function $L(r)$; r_0 is the radius of the unyielded core in fully-developed flow and $\bar{r}$ is the radius at which the fully-developed velocity is unity ($\bar{u}(\bar{r}) = 1$).

Development length	Definition
Classical or centerline development length [4]	$L_c \equiv L(0)$
Wall development length [14]	$L_w \equiv L(1)$
Viscoplastic development length as defined by Ookawara et al. [9]	$L_{95} \equiv L(0.95 r_0)$
Accelerating region development length (present work)	$L_m \equiv \max_{0 \le r \le \bar{r}} L$
Global development length (present work)	$L_g \equiv \max_{0 \le r \le 1} L$

pastes, foodstuff, pharmaceutical products, biofluids, etc [19,20]. Yield stress fluids behave like solids when they are not sufficiently stressed and flow like fluids when the yield stress, τ_0^*, is exceeded. Viscoplastic behavior is thus described by two-branch constitutive equations, the simplest of which is the Bingham-plastic equation [21]:

$$\begin{cases} \dot{\boldsymbol{\gamma}}^* = \mathbf{0}, & \tau^* \le \tau_0^* \\ \boldsymbol{\tau}^* = \left(\dfrac{\tau_0^*}{\dot{\gamma}^*} + \mu^* \right) \dot{\boldsymbol{\gamma}}^*, & \tau^* > \tau_0^* \end{cases} \tag{4}$$

where $\boldsymbol{\tau}^*$ is the stress tensor, μ^* is the plastic viscosity, and $\dot{\boldsymbol{\gamma}}^*$ is the rate-of-strain tensor. The latter is defined by

$$\dot{\boldsymbol{\gamma}}^* \equiv \nabla^* \mathbf{u}^* + (\nabla^* \mathbf{u}^*)^T \tag{5}$$

where $\mathbf{u}^*$ is the velocity vector and the superscript T denotes the transpose. The magnitudes of $\dot{\boldsymbol{\gamma}}^*$ and $\boldsymbol{\tau}^*$, denoted by $\dot{\gamma}^*$ and τ^*, are defined by $\dot{\gamma}^* \equiv \sqrt{\dot{\boldsymbol{\gamma}}^* : \dot{\boldsymbol{\gamma}}^*/2}$ and $\tau^* \equiv \sqrt{\boldsymbol{\tau}^* : \boldsymbol{\tau}^*/2}$, respectively. The Bingham model is reduced to the Newtonian model when the yield stress is zero. Other common viscoplastic constitutive models used in the literature include the Herschel-Bulkley and Casson models [22].

In flows of an ideal yield-stress fluid, i.e. of a fluid obeying a constitutive equation with two distinct branches, the flow domain consists of the so-called unyielded ($\tau^* \le \tau_0^*$) and yielded regions ($\tau^* > \tau_0^*$) where the two branches of the constitutive equation apply. Unyielded regions include zones where the material moves undeformed as a rigid body and dead zones where it is stagnant. Determining these regions is a key computational challenge with viscoplastic fluid flows, especially in two- and three-dimensional flows [23]. This issue is resolved by using the Augmented Lagrangian Methods (ALMs) which are based on the variational formulation of the Navier-Stokes equations and employ optimization algorithms to determine the flow solution [23]. These methods are exact in the sense that they respect the discontinuous form of the constitutive equation. However, they are generally slower and more difficult to implement than regularization methods [23], which are discussed below.

An alternative approach is to use the so-called regularization methods in which the constitutive equation is actually modified by introducing an additional parameter in order to combine the two branches of Eq. (4) into one smooth function, so that the resulting regularized equation applies everywhere in the flow field in both yielded and (practically) unyielded regions. The most popular regularization in the literature is that proposed by Papanastasiou [24]:

$$\boldsymbol{\tau}^* = \left\{ \frac{\tau_0^* [1 - \exp(-m^* \dot{\gamma}^*)]}{\dot{\gamma}^*} + \mu^* \right\} \dot{\boldsymbol{\gamma}}^* \tag{6}$$

where m^* is the stress growth exponent, which has dimensions of time. For sufficiently large values of m^* the Papanastasiou model provides a satisfactory approximation of the Bingham-plastic model. The regularized approach is easier to implement but

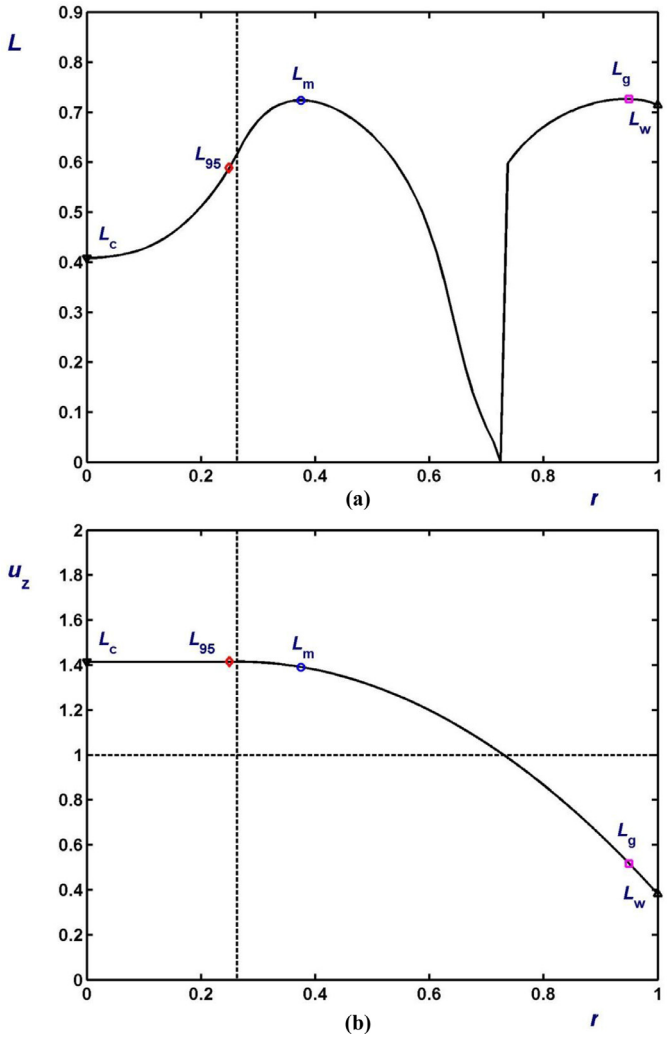

Fig. 2. Definitions of various development lengths. (a) The development length as a function of the radial distance for $Re = 0$, $Bn = 2$, and $B = 20$. (b) The fully-developed velocity profile. The vertical line corresponds to the yield point and the symbols denote the radial positions at which the various development lengths, L_c, L_{95}, L_m, L_g and L_w, are calculated.

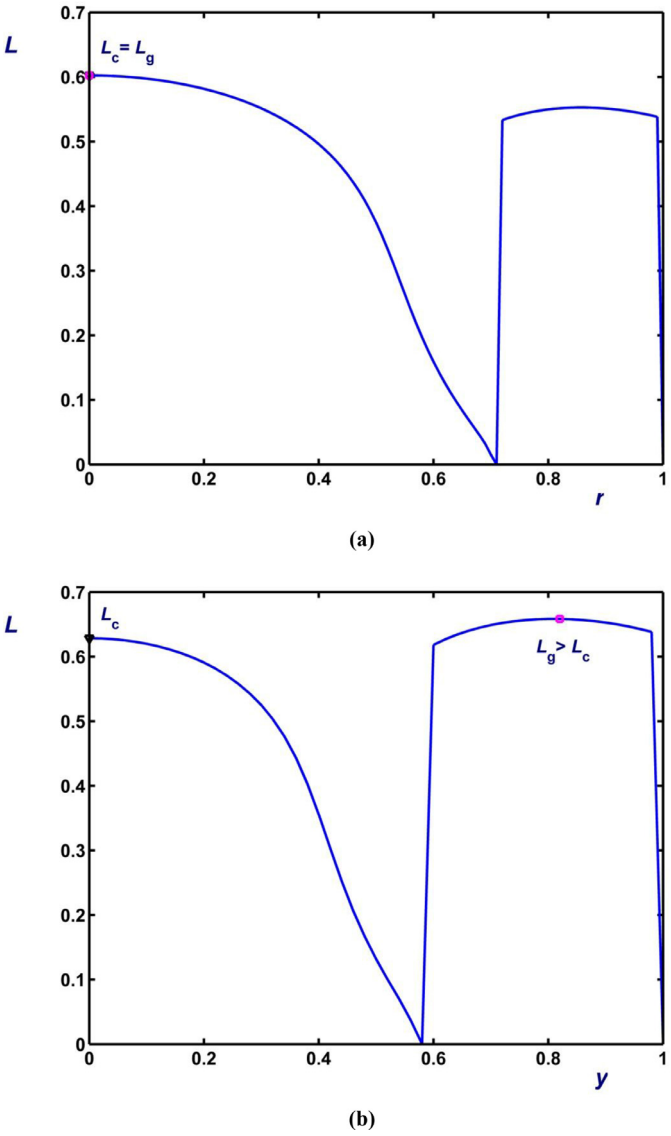

Fig. 3. The development length as a function of the transversal coordinate in the case of creeping ($Re = 0$) Newtonian flow with no wall slip: (a) Axisymmetric flow; (b) Planar flow. The classical development length L_c coincides with the global development length, L_g, only in the axisymmetric flow.

eliminates yield surfaces replacing unyielded regions with regions of very high viscosity. The interface of yielded /"unyielded" regions can approximately be tracked down a posteriori by using the von Mises criterion $\tau^* = \tau_0^*$ [20]. The advantages and disadvantages of ALMs and regularization methods have been recently reviewed by Balmforth et al. [23].

Wilson and Taylor [25] noted that in the case of an ideal discontinuous yield-stress fluid the entry flow is kinematically impossible and argued that to permit the flow development of a yield stress fluid, the usual ideal (discontinuous) models must be relaxed to permit some deformation of the unyielded material. Hence, regularizing the constitutive equation seems to be appropriate. In their analysis of the channel entry problem, Wilson and Taylor employed the biviscosity model [25]. Subsequently, Al Khatib and Wilson [26] calculated the approach to parallel flow by means of decaying eigenfunctions and showed that as the biviscosity model approaches the ideal Bingham model the approach to parallel flow becomes infinitely delayed.

Early works on viscoplastic flow development were concerned with high Reynolds number flows, i.e., they ignored the diffusion-dominated case [10]. These were also based on the use of the classical centerline development length L_c. It was thus incorrectly predicted that the development length vanishes in creeping flow. The use of L_c also lead to the wrong conclusion that the flow develops faster as the Bingham number is increased. For example, Vradis et al. [27] used an iterative finite difference technique on a staggered grid to solve Bingham plastic flow development in a pipe and reported that the velocity profiles develop faster with higher values of the yield stress, which "is to be expected given the increase of the core radius." Similarly, Dombrowski et al. [28] studied the entry flow of a Bingham plastic in a pipe for values of the yield stress such that the relative plug radius is in the range from 0.5 to 0.9 and reported that the classical development length is much shorter than that of a Newtonian fluid.

Ookawara et al. [9] were the first to observe that the flow near the centerline develops much faster than near the yield point. They thus proposed an alternative definition for the development length as the axial distance required for the velocity to reach 99% of the calculated maximum value at a radial location corresponding to 95% of the plug radius. We will introduce the symbol L_{95} for that development length. Ookawara et al. [9] justified their choice by

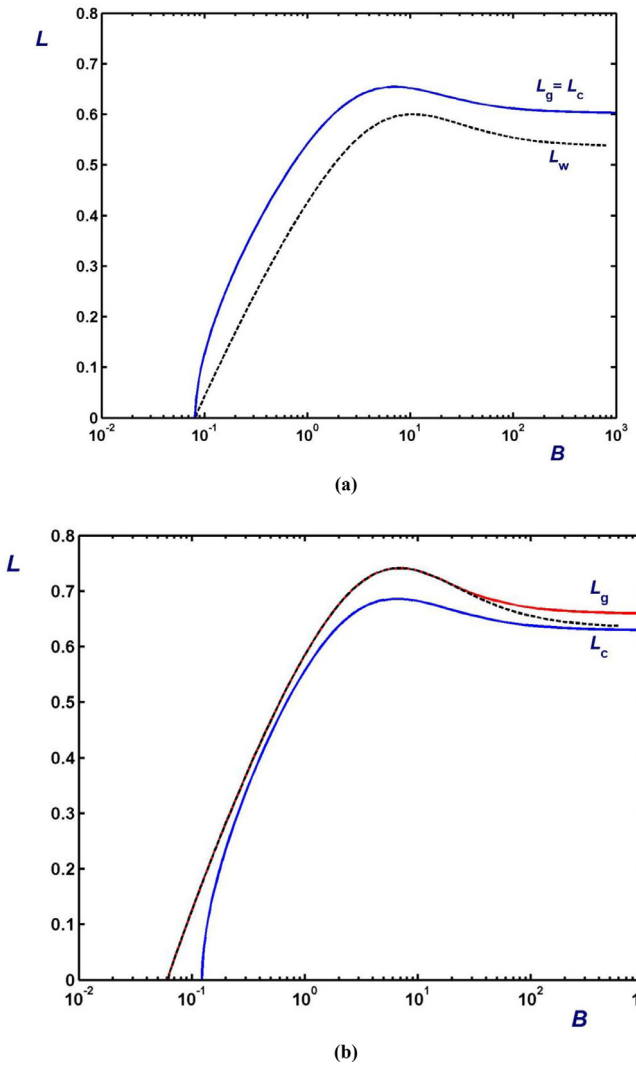

Fig. 4. Global, centerline, and wall (dashed) development lengths in Newtonian flow as functions of the slip number: (a) Axisymmetric flow; (b) Planar flow. The classical development length L_c coincides with the global development length L_g only in the axisymmetric flow. In the planar flow L_g coincides with L_w (which is always greater than L_c) only when slip is moderate or strong.

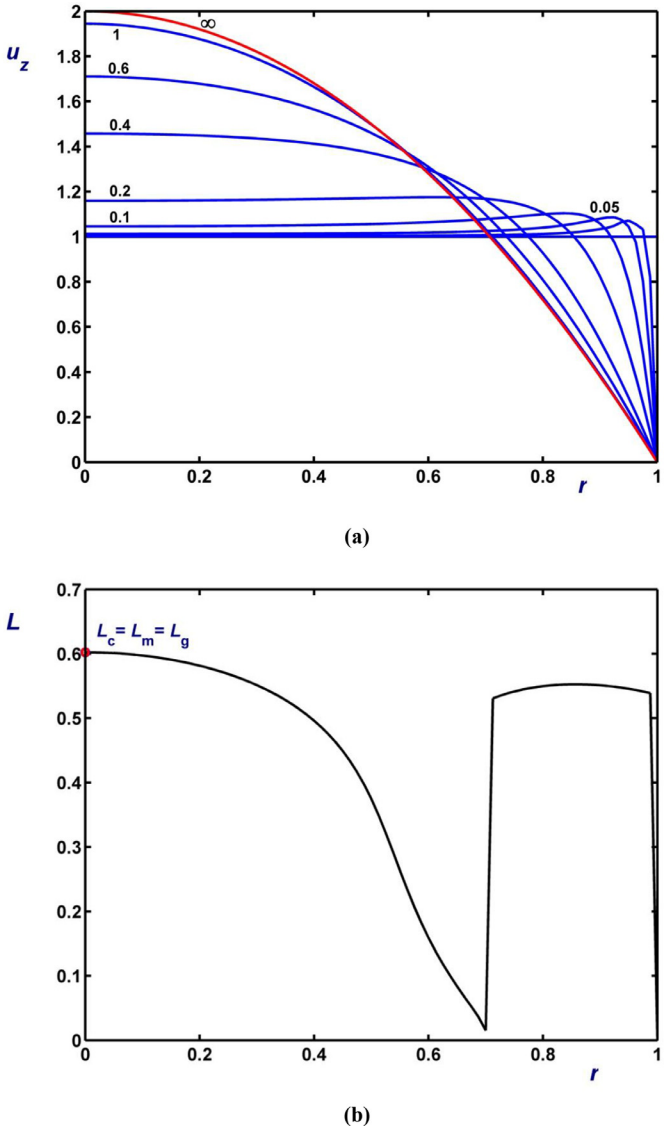

Fig. 5. Development of creeping Newtonian flow ($Bn = 0$) with no wall slip: (a) Velocity profiles at various axial distances; (b) Development length as a function of the radial distance. The classical, L_c, and the global development length, L_g, coincide in this case.

the inability to have a very fine mesh and thus a smooth velocity profile around the yield point due to numerical resources limitations and by the fact that the pressure gradient becomes constant beyond L_{95}. They also proposed a correlation according to which L_{95} is independent of the Bingham number at low Reynolds numbers.

Poole and Chhabra [10] pointed out that this result is unrealistic at low Reynolds numbers and carried out a systematic numerical investigation of the axisymmetric entry flow problem of a Bingham plastic for Bingham numbers in the range from 0 to 10. Their simulations, carried out with a commercial finite volume software using both the biviscosity and Papanastasiou models, showed that L_{95} is a weak non-monotonic function of the Bingham number exhibiting a minimum at low Reynolds numbers and is independent of the Bingham number at higher Reynolds numbers collapsing with the Newtonian (centerline) development length. Poole and Chhabra [10] did not pursue computations at higher Bingham numbers because convergence became increasingly difficult.

The objective of the present work is to study the development of viscoplastic flow in both pipes and channels at low and moderate Reynolds numbers in the presence of Navier slip and to test the dependence of the flow development on the Bingham number using alternative definitions of the development length. In addition to the development lengths already introduced, i.e. L_c, L_w and L_{95}, we also consider the global development length, L_g, as the maximum development length across the tube or the channel. The inclusion of slip is important given that viscoplastic materials are in general keen to slip (see [29] and references therein). Our finite element simulations for the no-slip case show that unlike L_{95} the global development length increases monotonically with the Bingham number. Moreover, for a given Bingham number, L_g increases with slip only initially passing from a global maximum beyond which it decreases rapidly to vanish at the full-slip limit which corresponds to sliding flow.

The rest of the paper is organized as follows. In Section 2, the governing equations for the axisymmetric flow are presented. In Section 3, the numerical method is briefly described and the numerical results are discussed. Finally, the main conclusions of this work are summarized in Section 4.

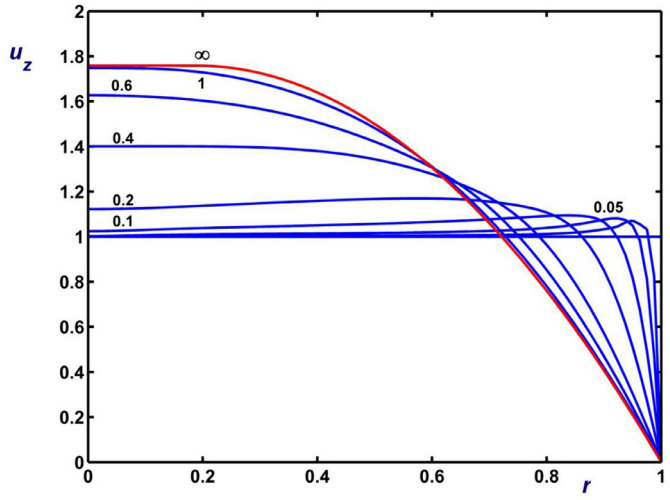

(a)

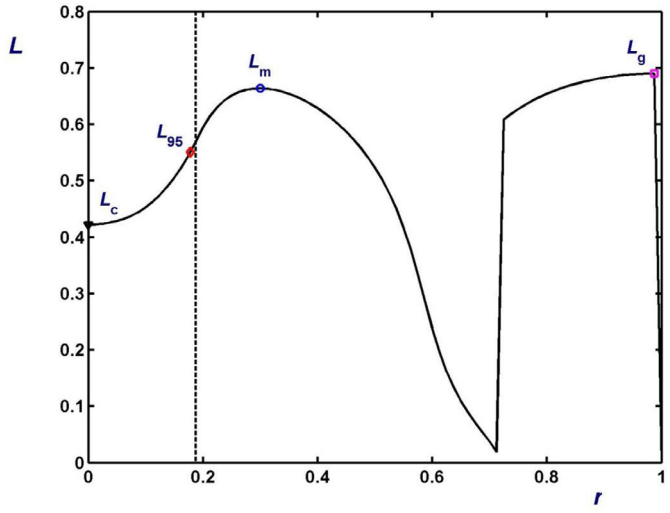

(b)

Fig. 6. Development of creeping Bingham flow ($Bn = 2$) with no wall slip: (a) Velocity profiles at various axial distances; (b) Development length as a function of the radial distance. The vertical line corresponds to the yield point and the symbols denote the radial positions at which the various development lengths, L_c, L_{95}, L_m, and L_g, are calculated.

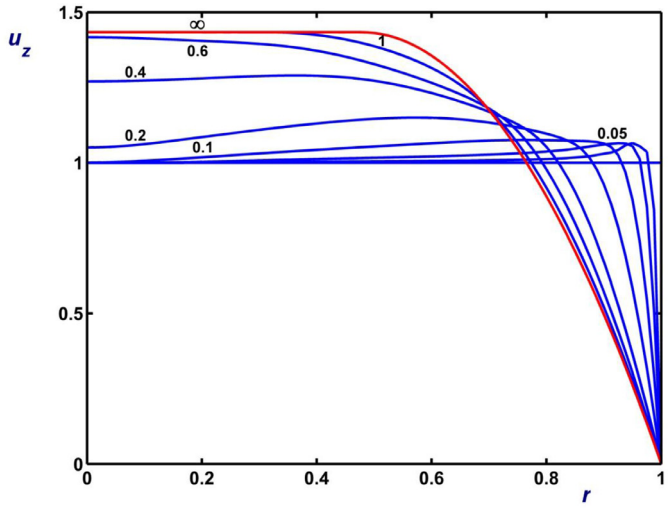

(a)

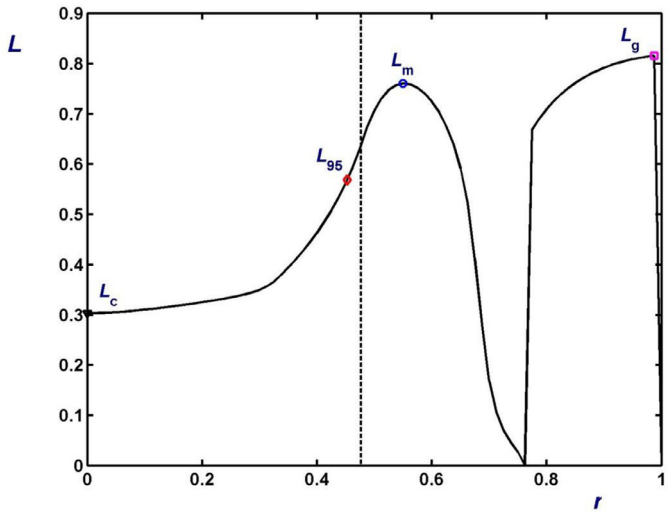

(b)

Fig. 7. Development of creeping Bingham flow ($Bn = 10$) with no wall slip: (a) Velocity profiles at various axial distances; (b) Development length as a function of the radial distance. The vertical line corresponds to the yield point and the symbols denote the radial positions at which the various development lengths, L_c, L_{95}, L_m, and L_g, are calculated.

2. Governing equations

Given that the equations for the two geometries of interest are analogous, only the equations for the axisymmetric entry flow are presented here. We consider the steady-state, laminar, incompressible Bingham-plastic flow development in a horizontal pipe of diameter $D^* = 2R^*$. The continuity equation and momentum equation are as follows

$$\nabla^* \cdot \mathbf{u}^* = 0 \tag{7}$$

and

$$\rho^* \mathbf{u}^* \cdot \nabla^* \mathbf{u}^* = -\nabla^* p^* + \nabla^* \cdot \boldsymbol{\tau}^* \tag{8}$$

where p^* is the pressure and ρ^* is the density, which is assumed to be constant. For the stress tensor $\boldsymbol{\tau}^*$, the Papanastasiou model (6) is employed instead of the ideal Bingham-plastic model (4).

A schematic of the computational domain along with the boundary conditions of the flow is shown in Fig. 1. At the inlet plane, the axial velocity is uniform, $u_z^* = U^*$, and the radial velocity component is set to zero, $u_r^* = 0$. The standard symmetry conditions for zero radial velocity and shear stress along the axis of symmetry are assumed. Along the pipe wall, the radial velocity is set to zero (no penetration) and the axial velocity obeys Navier's slip condition (3). The exit plane is taken sufficiently far downstream so that the flow can be taken as fully developed, i.e., both the normal stress component and the radial velocity component vanish, $-p^* + \tau_{zz}^* = 0$ and $u_r^* = 0$.

In the case of a non-yield-stress fluid, there is no bound on the permissible values of β^*. When $\beta^* = 0$, full slip is achieved in fully-developed Poiseuille flow. In the case of yield-stress fluids there exists a lower bound on the value of β^*, which depends on the yield stress. The fully-developed velocity in axisymmetric Poiseuille flow of a Bingham plastic is given by:

$$u_z^*(r^*) = u_w^* + \frac{G^*}{4\mu^*} \begin{cases} (R^* - r_0^*)^2, & 0 \le r^* \le r_0^* \\ \left[(R^* - r_0^*)^2 - (r^* - r_0^*)^2\right], & r_0^* \le r^* \le R^* \end{cases} \tag{9}$$

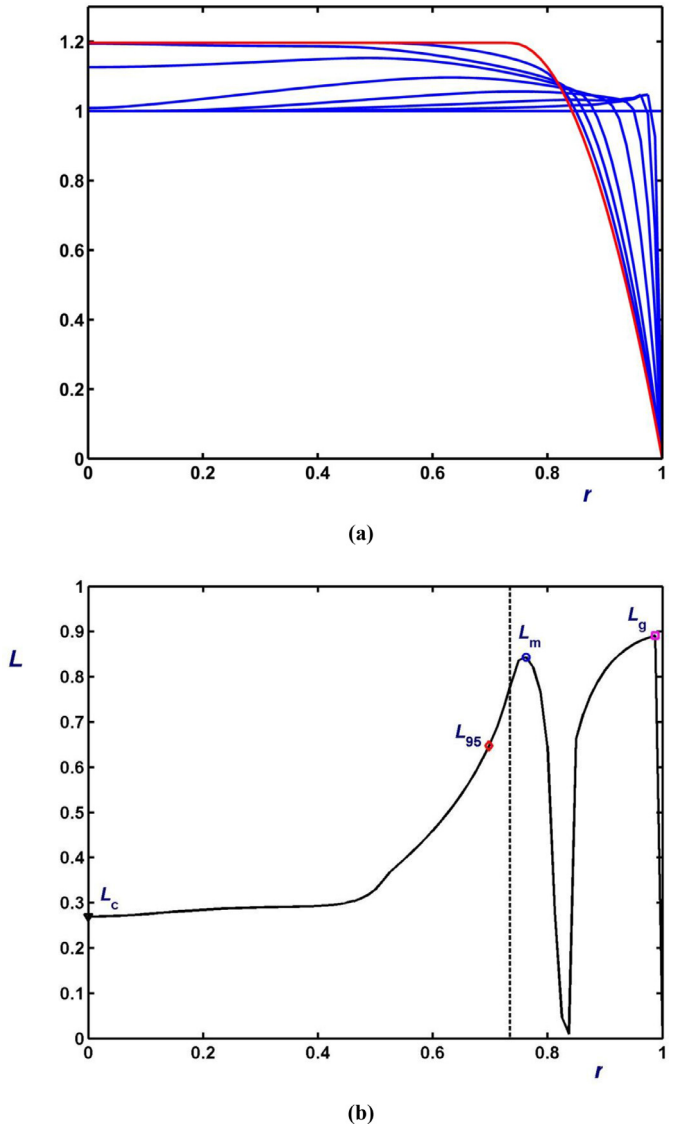

Fig. 8. Development of creeping Bingham flow ($Bn = 50$) with no wall slip: (a) Velocity profiles at various axial distances; (b) Development length as a function of the radial distance. The vertical line corresponds to the yield point and the symbols denote the radial positions at which the various development lengths, L_c, L_{95}, L_m, and L_g, are calculated.

where $G^* \equiv (-dp^*/dz^*)$is the imposed pressure gradient, u_w^* is the slip velocity, given by

$$u_w^* = \frac{R^* G^*}{2\beta^*} \tag{10}$$

and r_0^* is the yield point:

$$r_0^* = \frac{2\tau_0^*}{G^*} < R^* \tag{11}$$

It should be noted that when the pressure gradient is below $2\tau_0^*/R^*$, the axial velocity is uniform (sliding).

Scaling lengths by the pipe radius R^*, the velocity vector by the inlet velocity U^* and the pressure and the stress tensor components by $\mu^* U^*/R^*$, the governing equations are dedimensionalized as follows:

$$\nabla \cdot \mathbf{u} = 0 \tag{12}$$

and

$$\frac{1}{2} Re\, \mathbf{u} \cdot \nabla \mathbf{u} = -\nabla p + \nabla \cdot \boldsymbol{\tau}, \tag{13}$$

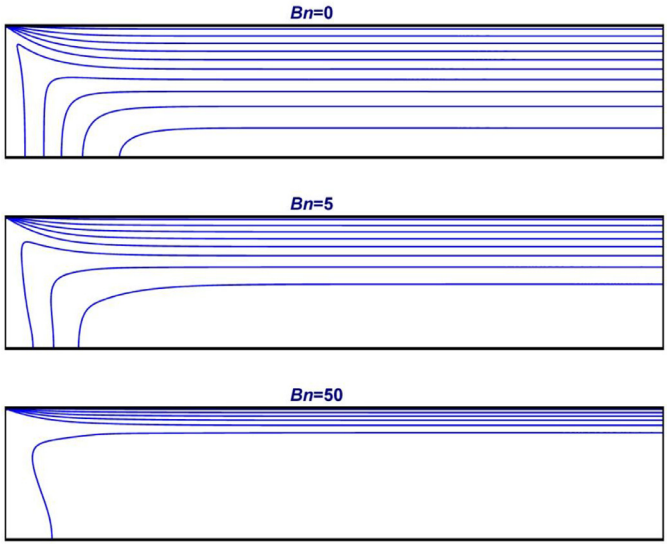

Fig. 9. Velocity contours (starting from 0.1 with a 0.2 step) in creeping axisymmetric flow with no wall slip ($B = \infty$) and $Bn = 0$ (Newtonian), 5 and 50.

where symbols without stars denote dimensionless variables and

$$Re \equiv \frac{2\rho^* U^* R^*}{\mu^*} \tag{14}$$

is the Reynolds number, based on the diameter, as in most other flow development studies [7,13].

Similarly, the dimensionless form of the Papanastasiou-regularized constitutive equation is

$$\boldsymbol{\tau} = \left[Bn \frac{1 - \exp(-M\dot{\gamma})}{2\dot{\gamma}} + 1 \right] \dot{\boldsymbol{\gamma}} \tag{15}$$

where

$$Bn \equiv \frac{2\tau_0^* R^*}{\mu^* U^*} \tag{16}$$

is the Bingham number (based on the diameter) and

$$M \equiv \frac{m^* U^*}{R^*} \tag{17}$$

is the dimensionless growth exponent.

The dimensionless form of the slip equation is

$$\tau_w = \frac{1}{2} B u_w \tag{18}$$

where

$$B \equiv \frac{2\beta^* R^*}{\mu^*} \tag{19}$$

is the slip number (based on the diameter, as in Ref. [7]).

The dimensionless fully-developed velocity profile is then

$$u_z(r) = u_w + \frac{G}{4} \begin{cases} (1 - r_0)^2, & 0 \le r \le r_0 \\ (1 - r_0)^2 - (r - r_0)^2, & r_0 \le r \le 1 \end{cases} \tag{20}$$

where $u_w = G/B$, $r_0 = Bn/G < 1$, and the dimensionless pressure gradient G is the root of the following equation, which is obtained by demanding that the dimensionless volumetric flow rate is equal to π:

$$24(1 - u_w)G^3 = (G - Bn)^2 \left(3G^2 + 2BnG + Bn^2\right) \tag{21}$$

It should be noted that for a given slip number, there is an upper bound for the Bingham number, which cannot be exceeded. This limiting value corresponds to the pressure gradient at which

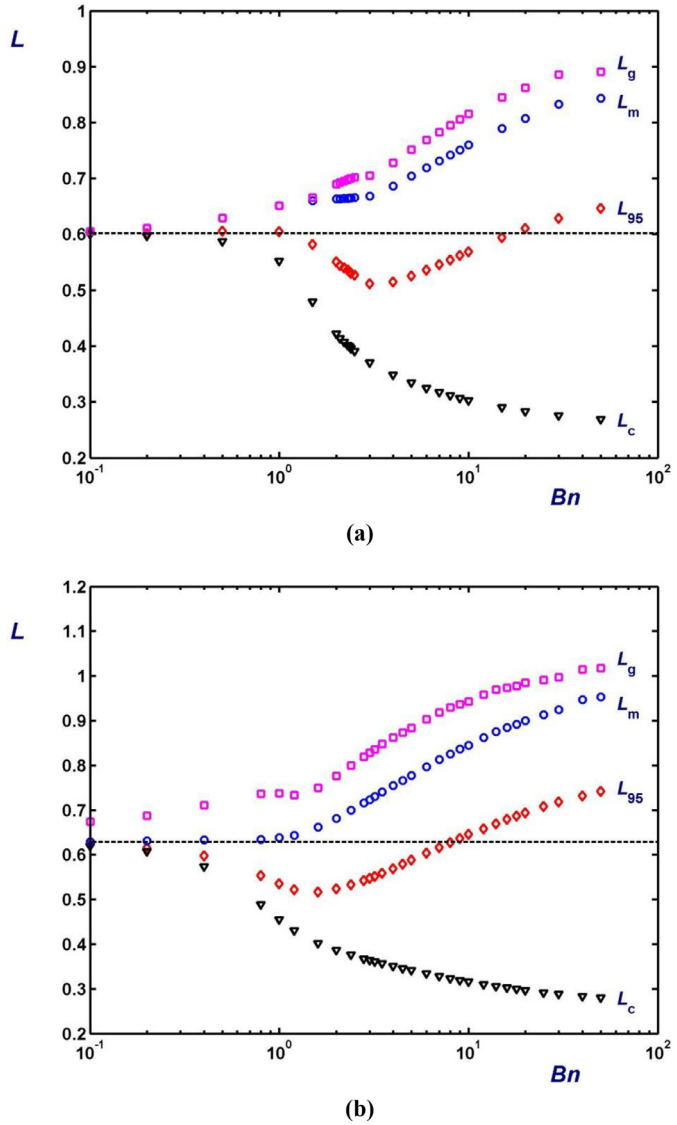

Fig. 10. Various development lengths (L_c, L_{95}, L_m and L_g) as functions of the Bingham number in creeping flow with no wall slip ($B=\infty$): (a) Axisymmetric flow; (b) Planar flow; The horizontal lines correspond to the classical (centerline) Newtonian development lengths ($L=0.6023$ and 0.6285, respectively).

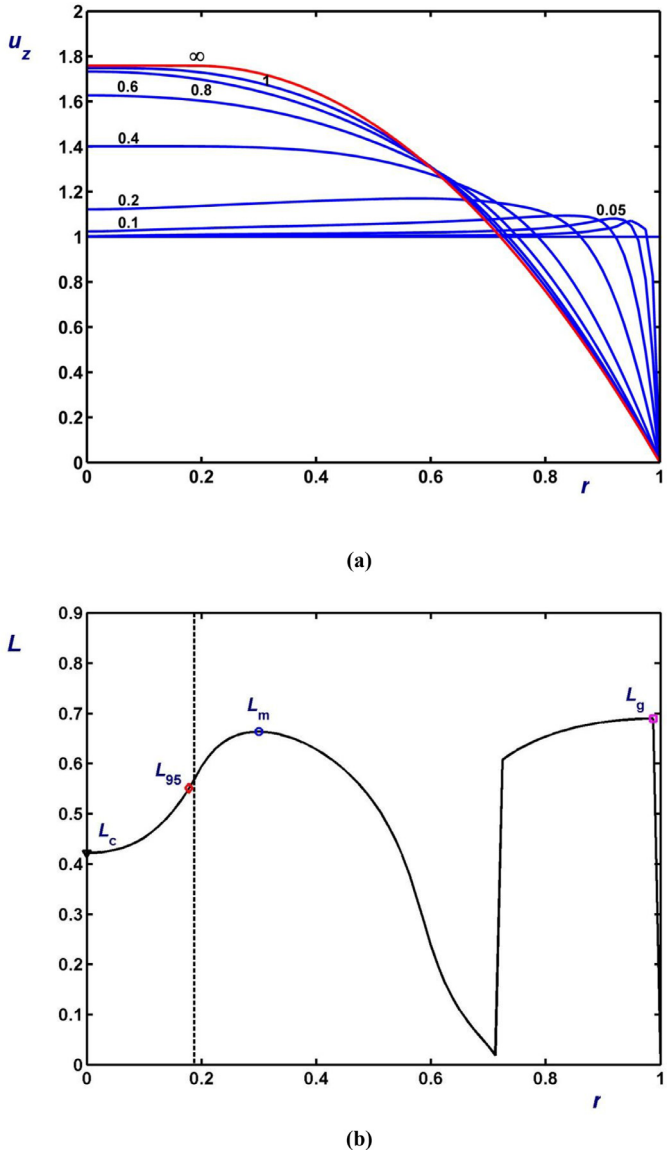

Fig. 11. Development of creeping axisymmetric flow for $Bn=2$ and no slip at the wall ($B=\infty$). (a) Velocity profiles at various axial distances; (b) The development length as a function of the radial distance. The vertical line corresponds to the yield point and the symbols denote the radial positions at which the various development lengths, L_c, L_{95}, L_m, and L_g, are calculated.

the fluid yields. From the above equation it is easily deduced that when Bn is equal to $Bn_{crit}=B$, both r_0 and u_w become 1 [30]. Similarly, for a given Bingham number the slip number should not be below Bn.

3. Numerical results and discussion

The system of the governing equations and the boundary conditions presented in Section 2 was solved numerically using the finite element method (u-v-p formulation) with standard biquadratic basis functions for the two velocity components and bilinear ones for the pressure field [14]. The Galerkin forms of the continuity and the momentum equations were used. The resulting nonlinear system of the discretized equations was solved using the Newton-Raphson iterative scheme and a standard frontal subroutine with a convergence tolerance equal to 10^{-4}.

Results have been obtained for Bingham numbers ranging from 0 (Newtonian flow) to 100, slip numbers in the range $[Bn, \infty)$, and Reynolds numbers up to 200. The convergence of the numerical results has been studied using both uniform and non-uniform meshes of different refinement and lengths. Table 1 shows the characteristics of four uniform (M1-M4) and four graded (GM1-GM4) meshes of length $L_{mesh}=20$ used in the present work. Graded meshes were more refined near the entry plane and near the wall; hence, the smallest element the size of which is provided in Table 1 was located at the upper left corner of the domain. As the Bingham and Reynolds numbers are increased, more refined and longer meshes are needed [10]. Given that we are mainly interested in low and moderate Reynolds number flows, using a mesh of length $L_{mesh}=20$ was found to be adequate for most of the results of this section. Results for $10 < Re \leq 200$ were obtained using a much longer mesh with $L_{mesh}=120$. Finally, the rather high value of $M=10^5$ for the regularization parameter has been used for most Bingham-plastic flow results of this section. The maximum value M_{max} of the growth parameter M at which the finite element code converges depends not only on the flow parameters, such as the Bingham, Reynolds and slip numbers, but also on the length of the computational domain and the mesh refinement. As

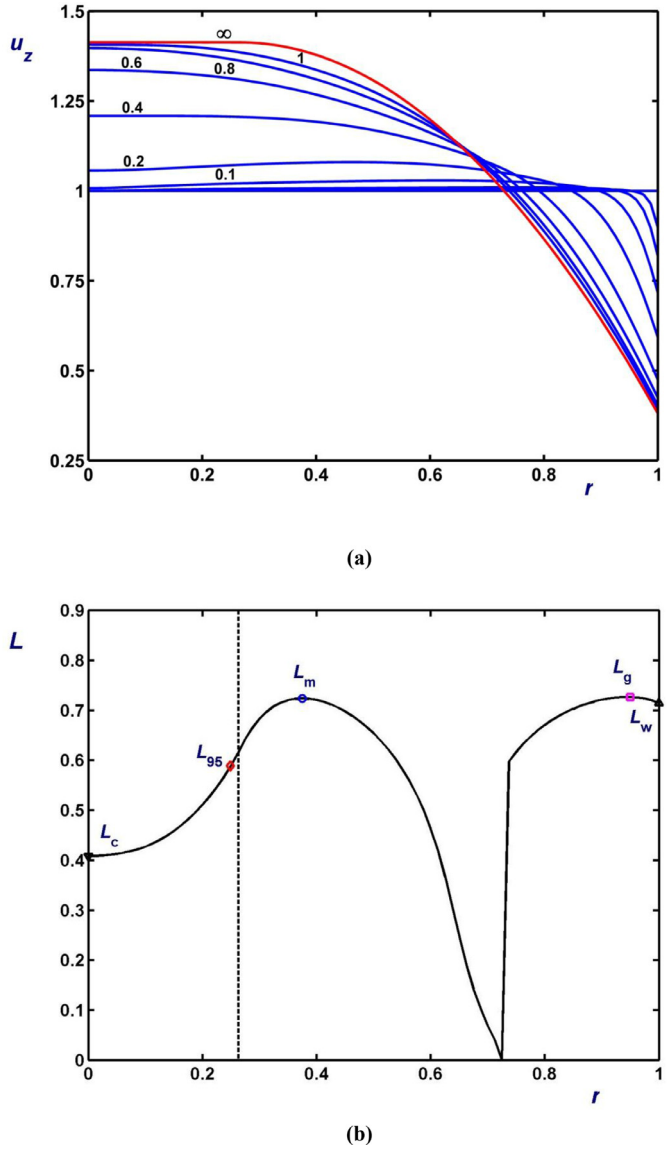

Fig. 12. Development of creeping axisymmetric flow for $Bn = 2$ and $B = 20$. (a) Velocity profiles at various axial distances; (b) The development length as a function of the radial distance. The vertical line corresponds to the yield point and the symbols denote the radial positions at which the various development lengths, L_c, L_{95}, L_m, L_g and L_w, are calculated.

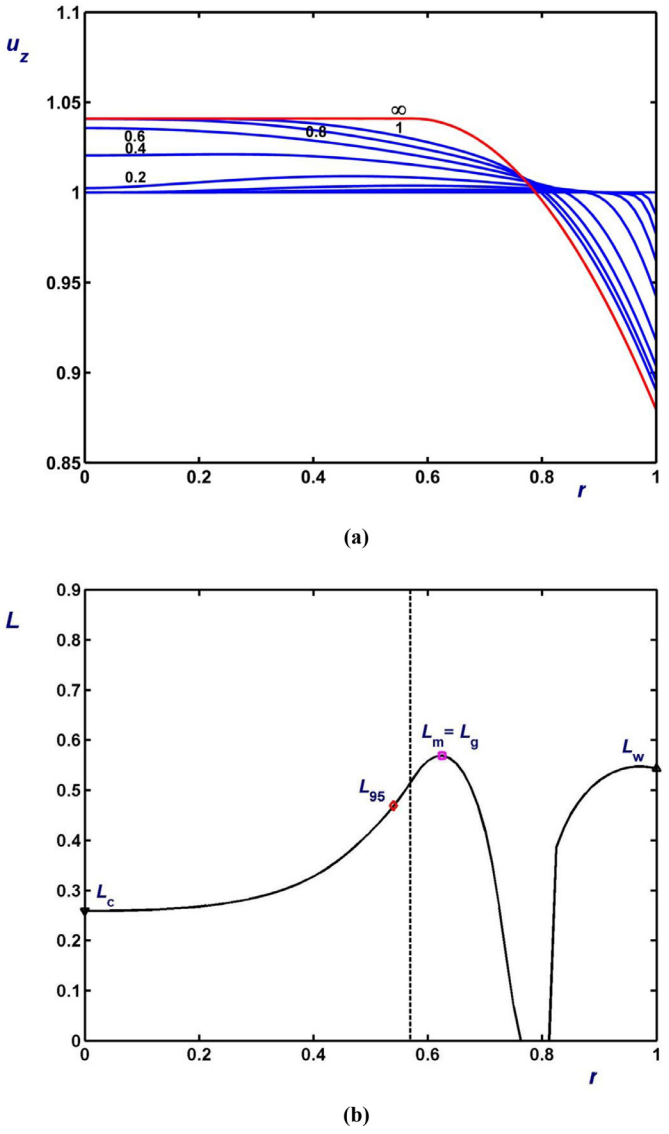

Fig. 13. Development of creeping axisymmetric flow for $Bn = 2$ and $B = 4$. (a) Velocity profiles at various axial distances; (b) The development length as a function of the radial distance. The vertical line corresponds to the yield point and the symbols denote the radial positions at which the various development lengths, L_c, L_{95}, L_m, L_g and L_w, are calculated.

an example, we take here the results for $Bn = 2$ and $Re = 0$ and 50, obtained with four uniform meshes M1-M4 with respective element sizes 0.2, 0.1, 0.05 and 0.25. In the case of creeping flow with no slip, the maximum value of the growth parameter was found to be $M_{max} = 10^6$ with M1-M3 while $M_{max} = 610^5$ with M4; in the case of slip with $B = 20$, $M_{max} = 10^6$ with M1, M2, and M4, while $M_{max} = 24{,}000$ with the rather coarse mesh M2. M_{max} is further reduced at higher values of the Reynolds number. When $Re = 100$ and no-slip is applied, the values of M_{max} with meshes M1-M4 were found to be 710^5, 310^5, 12,000 and 25,000, respectively, while with $B = 20$, the maximum values are $M_{max} = 10^6$ for M1 and M2 and M_{max}=3000 for M3 and M4. The latter value, which is the lowest one used in the present work, is still quite acceptable given that calculating yielded and unyielded regions is not of interest here [20,31]. It should also be noted that most of the results of this work have been obtained with graded and not uniform meshes, i.e. with meshes GM3 and GM4. Results concerning the convergence of the development length with mesh refinement and length are further discussed in the end of the section.

We have already encountered three different definitions for the development length: the classical or centerline development length L_c, the wall development length L_w, which is defined only if finite wall slip occurs, and L_{95} for viscoplastic flows [9]. As noted in [14], the wall development length has a meaning only in the presence of finite slip and below the critical value of the slip number at which 1% of the fully-developed slip velocity is equal to the convergence tolerance used in the numerical calculations. In Newtonian flow, the critical values of B are 792 and 594 for the axisymmetric and planar flows, respectively [14]. As discussed below, lower bounds for the slip number can be determined numerically as the values corresponding to full slip, i.e. to zero development length.

Obviously the development length is a function of the transversal coordinate, e.g., $L = L(r)$. If $\bar{u}(r)$ is the fully-developed velocity profile, then $L(r)$ is the length required by $u(r, z)$ to become equal to $0.99\bar{u}(r)$ or $1.01\bar{u}(r)$ when $\bar{u}(r) > 1$or $\bar{u}(r) < 1$, respectively. We hereby define as the global development length L_g the maximum value of L in the flow domain, $L_g \equiv \max_{0 \le r \le 1} L$. During flow

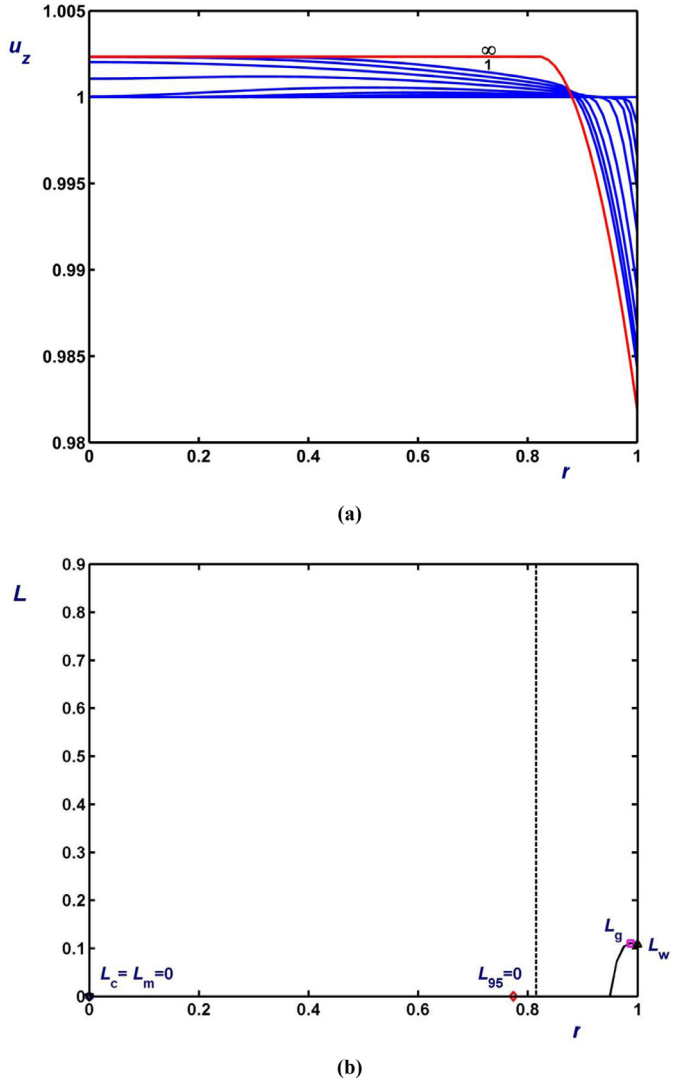

Fig. 14. Development of creeping axisymmetric flow for $Bn = 2$ and $B = 2.5$. (a) Velocity profiles at various axial distances; (b) The development length as a function of the radial distance. The vertical line corresponds to the yield point and the symbols denote the radial positions at which the various development lengths, L_c, L_{95}, L_m, L_g and L_w, are calculated.

development the fluid around the axis of symmetry accelerates in order to reach the fully-developed velocity; outside this region, the fluid decelerates in order to reach the fully-developed slip velocity. Obviously, the development length is zero at a critical value $\bar{r}$of the radius at which the dimensionless fully-developed velocity is unity. We will be using the symbol L_m for the maximum value of the L in the region where the fluid accelerates, i.e. $L_m \equiv \max_{0 \le r \le \bar{r}} L$. The definitions of all five development lengths considered in this work are tabulated in Table 2. They are also illustrated in Fig. 2, where we observe that L_m, i.e. the local maximum value of L in the accelerating region is not at the axis (or plane) of symmetry and does not necessarily coincide with the global development length L_g.

In Fig. 3, the Newtonian development lengths for creeping flow ($Re = 0$) with no-slip in both tubes and channels are plotted as a function of the transversal coordinate (r and y, respectively). We observe that the global development length coincides with the classical development length ($L_c = L_g$) only in the axisymmetric flow, which develops slower at the axis of symmetry. In the planar entry flow, $L_c < L_g$ which indicates that the flow develops more slowly in the decelerating region than in the accelerating one.

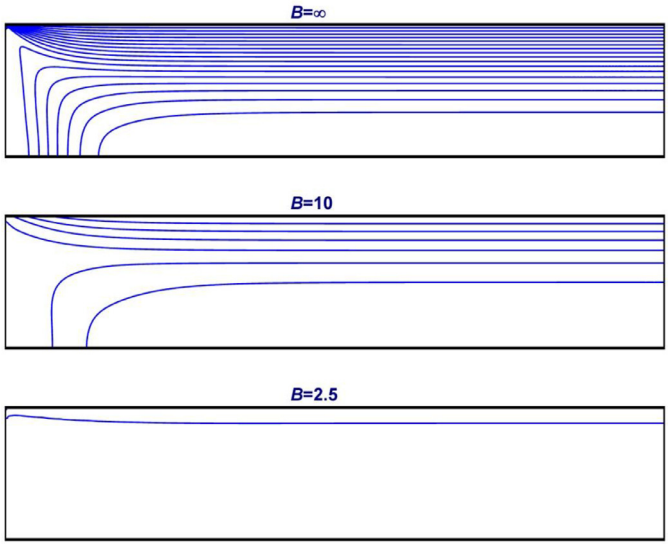

Fig. 15. Velocity contours (with a 0.1 step) in creeping axisymmetric Bingham flow with $Bn = 2$ and $B = \infty$ (no slip), 10 (moderate slip) and 2.5 (very strong slip).

Fig. 4 illustrates the effect of slip in the case of creeping Newtonian flow. In the axisymmetric flow (Fig. 4a) the maximum value of the development length is always at the axis of symmetry and thus $L_g = L_c$ for all the values of the slip number. The wall development length L_w is always much lower than the other two lengths. All lengths vanish at roughly the same slip number, $B_c \approx 0.082$, below which slip is very strong and the fully-developed velocity is practically flat. It should be noted that the wall development length is not defined above a certain critical value of the slip number (~ 792) at which slip is negligible. The results for the planar flow (Fig. 4b) differ from their axisymmetric counterparts in that the wall development length is always greater than the classical development length. In fact, L_w coincides with L_g for slip numbers lower than about 10, that is for moderate to very strong slip. When slip is weak, L_w lies between the classical and the global development lengths. As already noted by Kountouriotis et al. [14], L_w and L_c vanish at different critical slip numbers, i.e. ~0.06 and ~0.124, respectively. The maximum critical number at which L_w is defined is ~594.

Let us now move to the development of creeping ($Re = 0$) axisymmetric viscoplastic flow. The development of the flow for $Bn = 0$, 2, 10 and 50 is illustrated in Figs. 5–8, respectively, where the velocity profiles at different distances from the inlet are plotted. The function $L(r)$ is also plotted in each case with marks at the points where the development lengths of interest are computed. $L(r)$ exhibits two maxima which are always in the yielded region of the fully-developed velocity. Therefore, using L_c and L_{95} leads to a considerable underestimation of the development length. This can also be seen by examining more carefully the development of the axial velocity in the yielded regime in Figs. 6a, 7a and 8a. In general, L_{95} and L_c are much lower than L_m and L_g and the velocity overshoots diminish with increasing Bingham number, in agreement with the earlier observations of Vradis et al. [27] and Poole and Chhabra [10]. Looking more carefully, we see that while L_g increases monotonically, L_c decreases monotonically, and L_{95} initially decreases and then increases with the Bingham number. In other words, at higher Bingham numbers the axial velocity develops much faster near the axis of symmetry (i.e. in the region corresponding to the unyielded regime of the fully-developed flow) and more slowly near the wall (note that the scales of the verticals axes in Figs. 5–8aa are not the same). This phenomenon is also observed in Fig. 9, where the velocity contours computed for $Bn = 0$ (Newtonian flow), 5 and 50 are plotted. Hence, the development length

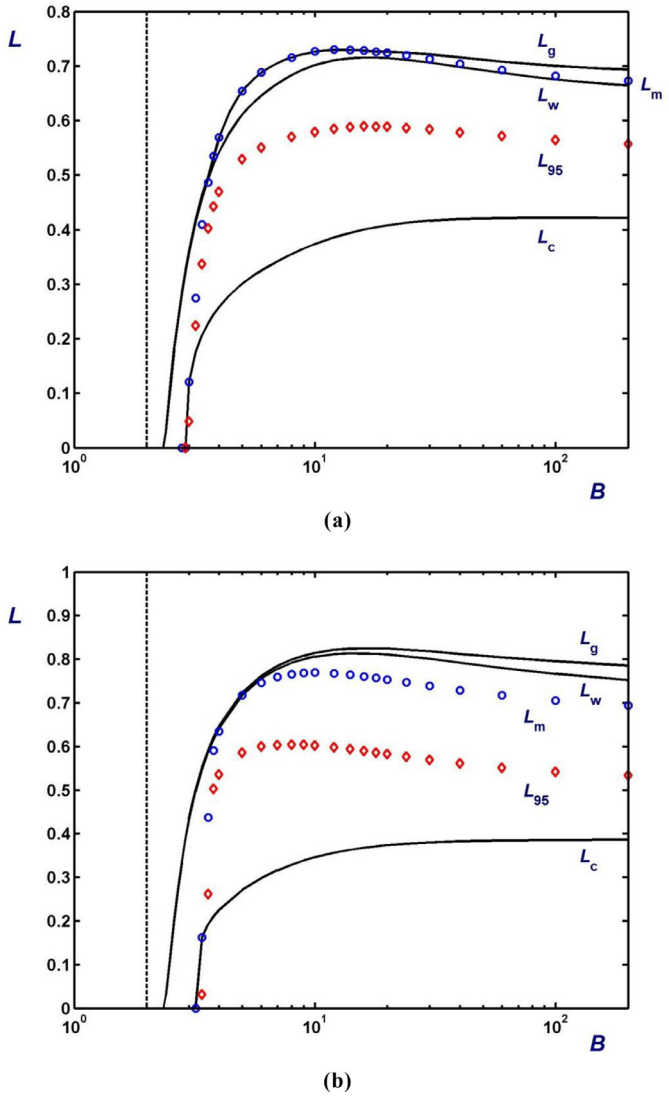

Fig. 16. Classical (L_c), wall (L_w) and global (L_g) development lengths as functions of the slip number for creeping axisymmetric flow with $Bn = 2$: (a) axisymmetric flow; (b) planar flow. L_m (circles) and L_{95} (diamonds) are also plotted. The vertical line at $B = Bn = 2$ corresponds to sliding flow at which the theoretical development length is exactly zero. However, due to its definition, L_g vanishes at a slightly higher slip number ($B \approx 2.4$ in the axisymmetric flow and $B \approx 2.3$ in the planar flow). Other development lengths vanish at a higher value of the slip number.

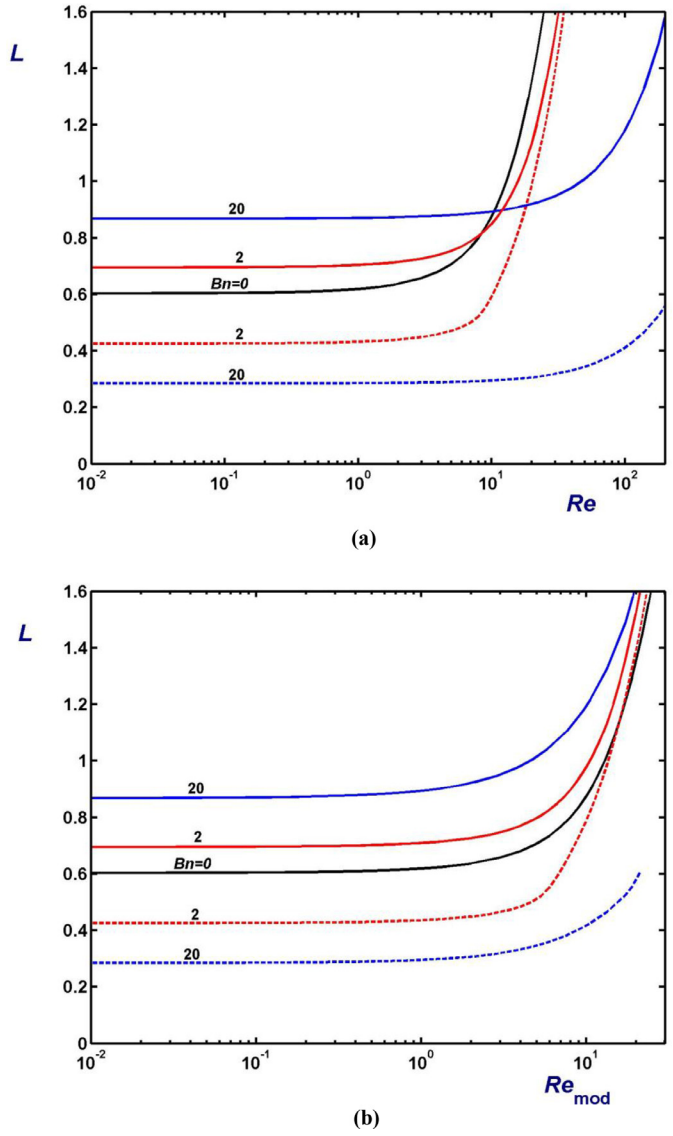

Fig. 17. Global (solid) and classical (dashed) development lengths in axisymmetric flow for $Bn = 0$ (Newtonian), 2 and 20: (a) versus the standard Reynolds number; (b) versus the modified Reynolds number.

should be defined carefully in order to assure flow development in the entire cross section of the tube. As the Bingham number is increased, the unyielded region of the fully-developed flow increases and so does the accelerating region of the flow. However, as it can be seen in Fig. 9, the magnitude of that acceleration is reduced, as the plug velocity approaches unity. Hence, the velocity contours are squeezed near the wall, while the central concavity of the contours observed near the entrance becomes more pronounced.

The various development lengths are plotted versus the Bingham number in Fig. 10 for both the axisymmetric and planar flows (recall that L_w is not defined in the case of no- or weak slip). We observe that the classical development length decreases monotonically and that L_{95} exhibits a minimum in both cases. Our results for the axisymmetric flow are in good agreement with the five values reported by Poole and Chhabra [10] for Bingham numbers in the range between 1 and 10. However, both L_m and L_g are increasing functions of the Bingham number, with the exception of a mild nonmonotonicity of L_{95} in the planar case for Bn around unity. Therefore, L_c and L_{95} are not safe indicators of flow development. The fact that L_g in the planar case is much higher than the other development lengths for low Bingham numbers is expected, since L_g does not coincide with L_c. All other development lengths for $Bn < 0.1$ are practically indistinguishable from the Newtonian result for L_c. A similar result has been reported by Poole and Chhabra [10] for L_{95} in the axisymmetric case.

In order to investigate the effect of slip we fixed the Bingham number to $Bn = 2$ and obtained results for different values of the slip number B. Figs. 11–14 show the evolution of the velocity in the case of creeping flow ($Re = 0$) for $B = \infty$ (no-slip), 20, 4, and 2.5 (recall that the lowest admissible value for the slip number is $B = Bn = 2$). As with the no-slip case, the two maxima of $L(r)$ are in the yielded region of the fully-developed axial velocity. We note that the classical development length L_c decreases with slip and eventually becomes zero. When slip is strong, i.e., at low values of the slip number the flow is practically developed in the unyielded regime but flow still needs to develop near the wall. With increasing slip the velocity tends to become plug, which is the case when the slip number is equal to the Bingham number. In such

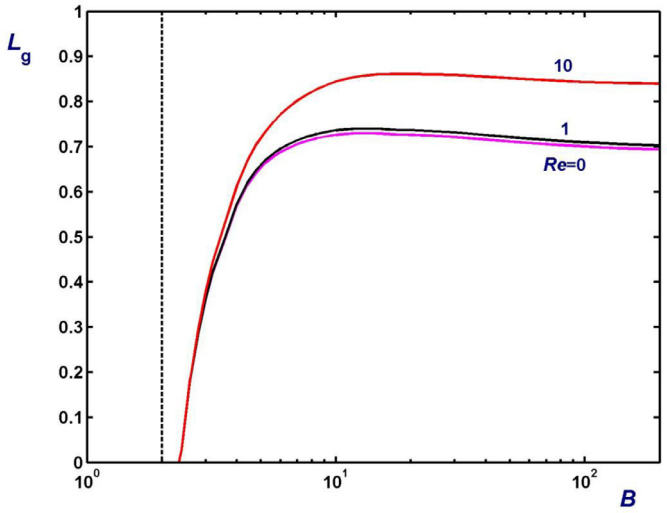

Fig. 18. Global development length as a function of the slip number for $Bn = 2$ and various Reynolds numbers. The vertical line at $B = Bn = 2$ corresponds to sliding flow at which the theoretical development length is exactly zero. However, due to its definition, L_g vanishes at a slightly higher slip number, $B \approx 2.4$.

a case the development length is zero. Note that slip suppresses the velocity overshoots. We also see that the wall and global development lengths are similar. Fig. 15 shows the velocity contours computed for $Bn = 2$ and three different values of the slip number: $B = \infty$ (no-slip), 10, and 2.5. As the slip number is reduced, the flow field approaches more the sliding flow, which in theory is achieved when $B = Bn = 2$. Hence the contours become sparser and their central concavity near the entrance weakens with slip.

In Fig. 16, we plotted the various development lengths versus the slip number for both the axisymmetric and planar flows when $Bn = 2$ and $Re = 0$. Recall that no-slip corresponds to $B = \infty$ and that sliding flow corresponds to $B = Bn = 2$. In the latter case the theoretical development length is obviously zero. Due to its definition, the global development length L_g vanishes at a slightly higher slip number, i.e. $B \approx 2.4$ for the axisymmetric and $B \approx 2.3$ for the planar case. This is also the case for L_w, while L_c, L_{95} and L_m vanish at a higher value (~2.9). We observe that the classical development length L_c is always much lower than the other development lengths and vanishes at a higher value of the slip number. Moreover, it is the only one that increases monotonically with the slip number, while all the others exhibit a maximum. For both the axisymmetric and planar geometries, the values of L_{95} are roughly between L_c and L_g. Again L_c and L_{95} are not safe indicators for viscoplastic flow development.

To investigate the effect of inertia on the flow development of the axisymmetric Bingham flow in the absence of slip, we obtained results for three different Bingham numbers, $Bn = 0$, 2, and 10, and Reynolds numbers ranging from 0 up to 200. The global and the centerline development lengths are plotted versus the Reynolds number in Fig. 17a. As already noted the difference between L_g and L_c is zero in Newtonian flow ($Bn = 0$) and increases with the Bingham number. This difference increases initially with the Reynolds number and then tends to reduce at higher Reynolds numbers (see the results for $Bn = 2$). What may be striking is that the increase of the global development length with the Bingham number is observed only at low Reynolds numbers and that for Re above 10 (where the curves cross) the opposite effect is observed. This change in the effect of the Bingham number is not observed if instead of using the standard definition of the Reynolds number in Eq. (14) one employs the following modified Reynolds number, which is based on the momentum correction coefficient method

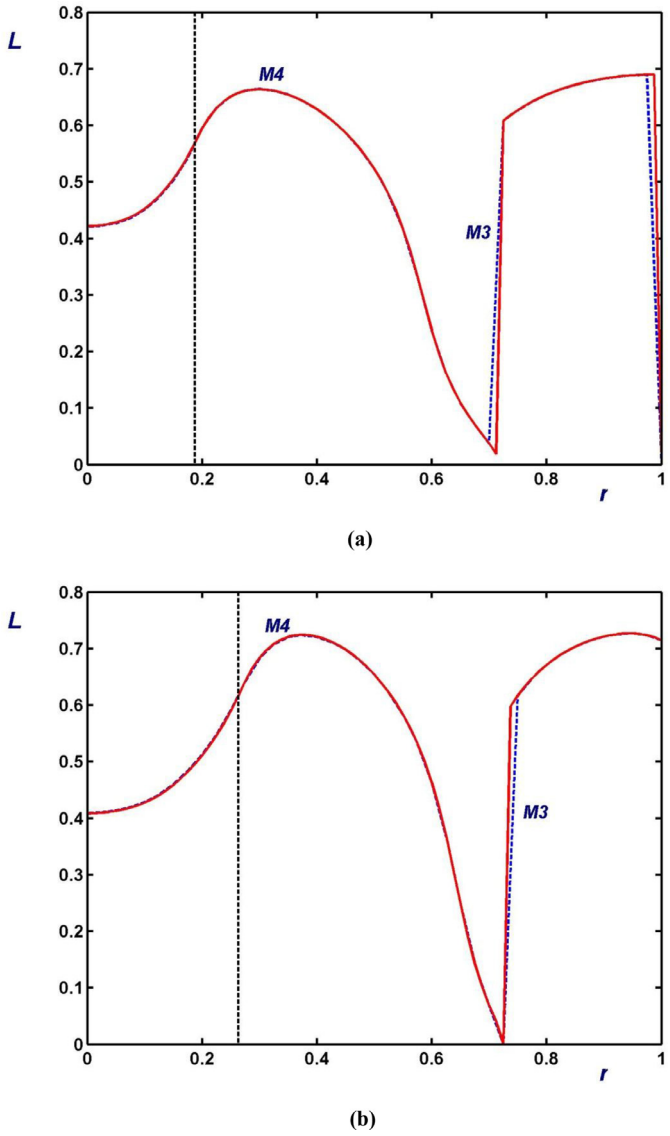

Fig. 19. Global development lengths for creeping, axisymmetric Bingham flow flow with $Bn = 2$ calculated with uniform meshes M3 (dashed) and M4 (solid): (a) $B = \infty$ (no slip); (b) $B = 20$. The vertical lines indicate the position of the yield point ($r_0 = 0.18758$ and 0.26280, respectively).

suggested by Ito (see [9] and references therein):

$$Re_{\text{mod}} = \zeta Re \tag{22}$$

where

$$\zeta = \frac{3(5 + 6r_0 - 11r_0^2)(r_0^4 - 4r_0 + 3)}{5(3 + 2r_0 + r_0^2)^2} \tag{23}$$

$r_0 = Bn/G$ is the radius of the unyielded region in fully-developed flow, and G is the root of Eq. (21). It is clear that in Newtonian flow (r_0=0) Re_{mod} is identical to Re. The values of ζ for $Bn = 2$ and 20 are found to be 0.66636 (r_0=0.18758) and 0.09612 ($r_0 = 0.60222$), respectively. Replotting L_g and L_c versus the modified Reynolds number (Fig. 17b) reveals that the development length is an increasing function of the Bingham number in the range of Reynolds numbers considered here. Moreover, at higher Reynolds numbers all curves tend to collapse to the Newtonian data, as it was also pointed out by Poole and Chhabra [10]. The latter authors reported that below a critical Reynolds number (of about 40 for a Bingham number equal to 10) L_{95} departs from the Newtonian correlation in

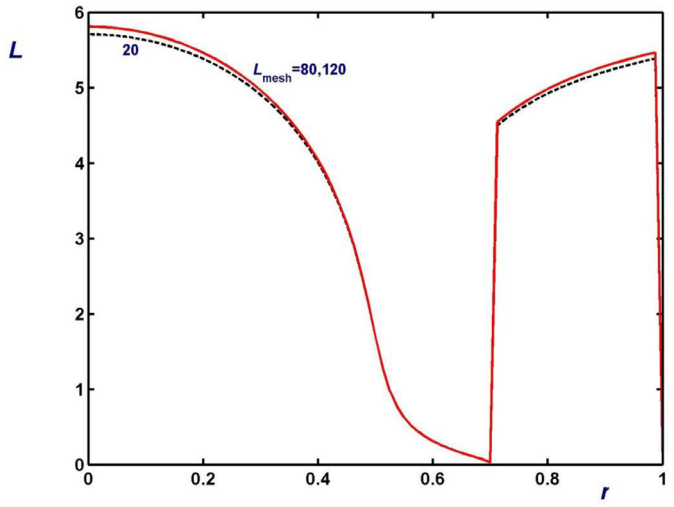

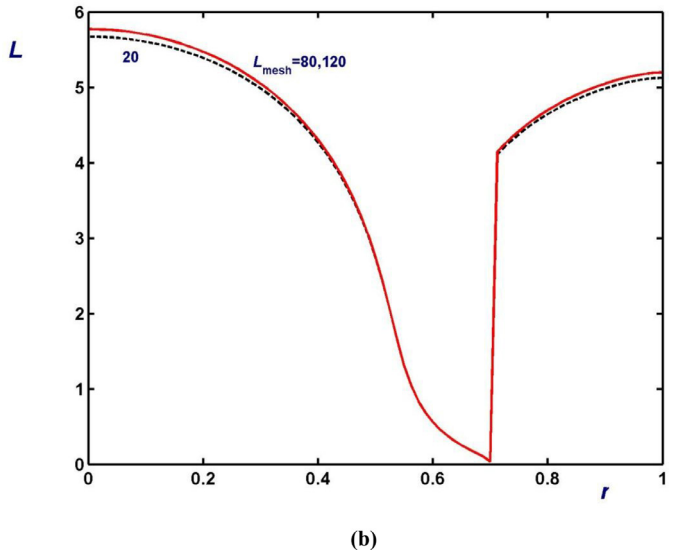

Fig. 20. Global development lengths for creeping, axisymmetric Newtonian flow with $Re = 100$ calculated with uniform meshes of different length L_{mesh}: (a) $B = \infty$ (no slip); (b) $B = 20$.

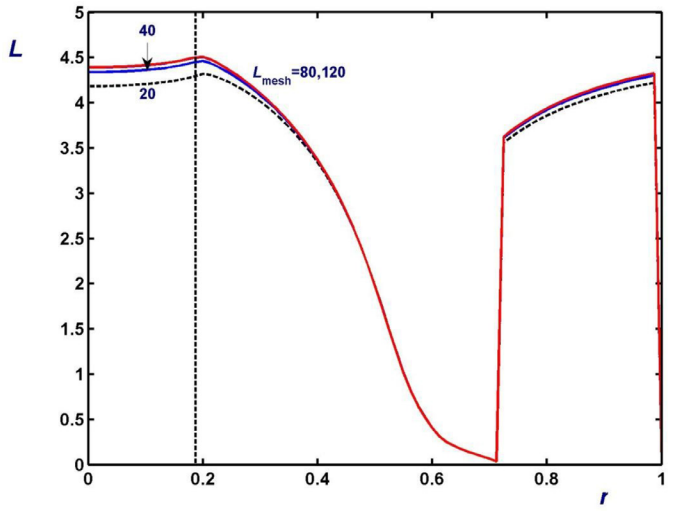

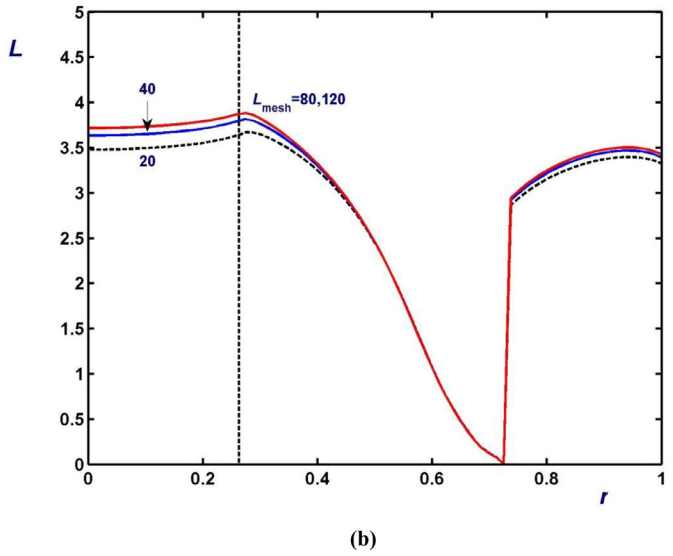

Fig. 21. Global development lengths for creeping, axisymmetric Bingham flow with $Bn = 2$ and $Re = 100$ calculated with uniform meshes of different length L_{mesh}: (a) $B = \infty$ (no slip); (b) $B = 20$. The vertical lines indicate the position of the yield point ($r_0 = 0.18758$ and 0.26280, respectively).

a non-monotonic fashion. However, the results of Fig. 17b demonstrate that L_g is a monotonically increasing function of the Bingham number in the range of momentum-corrected Reynolds numbers examined here.

The effect of inertia in the presence of slip is illustrated in Fig. 18, where the global development lengths for the axisymmetric flow with $Bn = 2$ and $Re = 0$, 1, and 10 are plotted. We observe that L_g increases with inertia and that this increase becomes less pronounced at low values of the slip number, i.e. when slip is strong. This was also true for all other development lengths considered in this work.

Finally, the convergence of the development length $L(r)$ with mesh refinement when $Bn = 2$, $Re = 0$ and $B = \infty$ (no slip) and 20, is illustrated in Fig. 19, where results obtained with uniform meshes M3 and M4 are shown. (We have chosen uniform instead of graded meshes so that the differences are visible.) The convergence with the length of the computational domain, L_{mesh}, for $Re = 100$ is illustrated in Figs. 20 and 21, where results for the Newtonian ($Bn = 0$) and a Bingham-plastic case ($Bn = 2$) are respectively shown. Interestingly, the effect of L_{mesh} appears to be more important in the Bingham flow even though the values of L_g in Fig. 21 for $B = \infty$ and 20 are lower than their Newtonian counterparts in Fig. 20. Moreover, the most pronounced differences are observed in the unyielded region of the fully-developed flow. Nevertheless, the length $L_{mesh} = 120$ was found to be adequate for all results presented here.

4. Conclusions

We have investigated the laminar flow development of yield stress fluids of the Bingham- plastics type in pipes and channels with wall slip by means of finite element simulations using the regularized Papanastasiou constitutive equation and considering alternative definitions of the development length. We have shown that the classical development length L_c and the development length proposed by Ookawara et al. [9] for Bingham flow (i.e., L_{95}) are not good choices for measuring viscoplastic flow development (with or without slip). The global development length, L_g, is monotonically increasing with the Bingham number, whereas L_{95} exhibits a minimum. The global development length increases initially with slip exhibiting a maximum and then decreases rapidly

vanishing when the value of the slip number is slightly above the Bingham number. Moreover, the velocity overshoots are suppressed by both slip and yield stress.

References

[1] M. Friedmann, J. Gillis, N. Liron, Laminar flow in a pipe at low and moderate Reynolds numbers, Appl. Sci. Res. 19 (1968) 426–438.
[2] B. Atkinson, M.P. Brocklebank, C.C.H. Card, J.M. Smith, Low Reynolds number developing flows, AIChE J. 15 (1969) 548–553.
[3] D. Fargie, B. Martin, Developing laminar flow in a pipe of circular cross-section, Procs. Royal. Soc. London A 321 (1971) 461–476.
[4] R. Shah, A. London, Laminar Flow Forced Convection in Ducts: a Source Book for Compact Heat Exchanger Analytical Data, Academic Press, New York, 1978.
[5] A. Sinclair, Steady and Oscillatory Flow in the Entrance Region of Microchannels PhD Thesis, The University of New South Wales, 2012.
[6] R.J. Poole, B.S. Ridley, Development-length requirements for fully developed laminar pipe flow of inelastic non-Newtonian liquids, ASME J. Fluids Eng 129 (2007) 1281–1287.
[7] L.L. Ferrás, A.M. Afonso, J.M. Nóbrega, M.A. Alves, F.T. Pinho, Development length in planar channel flows of Newtonian fluids under the influence of wall slip, ASME J. Fluids Eng 134 (2012) 104503.
[8] R.I. Tanner, Engineering Rheology, second ed., Oxford University Press, Oxford, 2000.
[9] S. Ookawara, K. Ogawa, N. Dombrowski, E. Amooie-Foumeny, A. Riza, Unified entry length correlation for Newtonian, power law and Bingham fluids in laminar pipe flow at low Reynolds numbers, J. Chem. Eng. Japan 33 (2000) 675–678.
[10] R.J. Poole, R.P. Chhabra, Development length requirements for fully developed laminar pipe flow of yield stress fluids, ASME J. Fluids Eng 132 (2010) 034501.
[11] K. Yapici, B. Karasozen, Y. Uludag, Numerical analysis of viscoelastic fluids in steady pressure-driven channel flow, ASME J. Fluids Eng. 134 (2012) 051206.
[12] L.L. Ferrás, C. Fernandes, O. Pozo, A.M. Afonso, M.A. Alves, J.M. Nóbrega, F.T. Pinho, Development length in channel flows of inelastic fluids described by the Sisko viscosity model, V Conferencia Nacional de Mecanica dos Fluidos, Termodinamica e Energia MEFTE 2014, 2014 11-12 September.
[13] F. Durst, S. Ray, B. Unsal, O.A. Bayoumi, The development lengths of laminar pipe and channel flows, ASME J. Fluids Eng 127 (2005) 1154–1160.
[14] Z. Kountouriotis, M. Philippou, G.C. Georgiou, Development lengths in Newtonian Poiseuille flows with wall slip, J. Fluids Eng. (2016).
[15] C. Neto, D.R. Evans, E. Bonaccurso, H.J. Butt, V.S. Craig, Boundary slip in Newtonian liquids: A review of experimental studies, Rep. Progr. Phys 68 (2005) 2859–2897.
[16] Ch. 19 E. Lauga, M.P. Brenner, H.A. Stone, in: C. Tropea, A.L. Varin, J.F. Foss (Eds.), Handbook of Experimental Fluid Dynamics, Springer, New York, 2007, pp. 1219–1240.
[17] C.L.M.H. Navier, Sur les lois du mouvement des fluids, Mem. Acad. R. Sci. Inst. Fr 6 (1827) 389–440.
[18] M.M. Denn, Extrusion instabilities and wall slip, Ann. Rev. Fluid Mech. 33 (2001) 265–287.
[19] H.A. Barnes, The yield stress—a review or '$\pi\alpha\nu\tau\alpha\ \rho\varepsilon\iota$— everything flows? J. non-Newtonian Fluid Mech 81 (1999) 133–178.
[20] E. Mitsoulis, Flows of viscoplastic materials; Models and computation, Rheology Reviews 2007 (2007) 135–178.
[21] E.C. Bingham, Fluidity and Plasticity, McGraw-Hill, New York, 1922.
[22] R.B. Bird, G.C. Dai, B.J. Yarusso, The rheology and flow of viscoplastic materials, Rev. Chem. Eng. 1 (1982) 1–70.
[23] N.J. Balmforth, I.A. Frigaard, G. Ovarlez, Yielding to stress: Recent developments in viscoplastic fluid mechanics, Annu. Rev. Fluid Mech 46 (2014) 121–146.
[24] T.C. Papanastasiou, Flows of materials with yield, J. Rheol 31 (1987) 385–404.
[25] S.D.R. Wilson, A.J. Taylor, The channel entry problem for a yield stress fluid, J. non-Newtonian Fluid Mech 65 (1996) 165–176.
[26] M.A.M. Al Khatib, S.D.R. Wilson, The development of Poiseuille flow of a yield--stress fluid, J. non-Newtonian Fluid Mech 100 (2001) 1–8.
[27] G.C. Vradis, J. Dougher, S. Kumar, Entrance pipe flow and heat transfer for a Bingham plastic, Int. J. Heat Mass Transfer 36 (1993) 543–552.
[28] N. Dombrowski, E.A. Foumeny, S. Ookawara, A. Riza, Characterisation of blood flow properties using CFD, in: C. Tayor (Ed.), Numerical Methods in Laminar and Turbuelent Flow, 13, Pineridge Press, Swansea, England, 1993, pp. 26–37.
[29] S. Aktas, D.M. Kalyon, B.M. Marín-Santibáñez, J. Pérez-González, Shear viscosity and wall slip behavior of a viscoplastic hydrogel, J. Rheol 58 (2014) 513–534.
[30] Y. Damianou, G.C. Georgiou, I. Moulitsas, Combined effects of compressibility and slip in flows of a Herschel-Bulkley fluid, J. Non-Newtonian Fluid. Mech 193 (2013) 89–102.
[31] Y. Damianou, G.C. Georgiou, Viscoplastic Poiseuille flow in a rectangular duct with wall slip, J. non-Newtonian Fluid Mech 214 (2014) 88–105.